Xia et al. BMC Biology (2025) 23:37
https://doi.org/10.1186/s12915-025-02142-w

BMC Biology

RESEARCH ARTICLE Open Access

CDK1 mediates the metabolic regulation of DNA double-strand break repair in metaphase II oocytes

Tian-Jin Xia[1,2], Feng-Yun Xie[1,2], Juan Chen[1,2], Xiao-Guohui Zhang[1,3], Sen Li[1,2], Qing-Yuan Sun[1,2], Qin Zhang[2*], Shen Yin[4*], Xiang-Hong Ou[1,2,3*] and Jun-Yu Ma[1,2,3*]

Abstract

Background During oocyte maturation, DNA double-strand breaks (DSBs) can decrease oocyte quality or cause mutations. How DSBs are repaired in dividing oocytes and which factors influence DSB repair are not well understood.

Results By analyzing DSB repair pathways in oocytes at different stages, we found that break-induced replication (BIR) and RAD51-mediated homology-directed repair (HDR) were highly active in germinal vesicle breakdown (GVBD) oocytes but suppressed in metaphase II (MII) oocytes and the BIR in oocytes was promoted by CDK1 activity. By culturing oocytes in different media, we found that high-energy media, such as DMEM, decreased CDK1 protein levels and suppressed BIR or HDR in MII oocytes. In contrast, 53BP1-mediated nonhomologous end joining (NHEJ) repair was inhibited in germinal vesicle (GV) and GVBD oocytes but promoted in MII oocytes, and NHEJ was not affected by DMEM medium and CDK1 activity. In addition, in DSB MII oocytes, polymerase theta-mediated end joining (TMEJ) was found to be suppressed by CDK1 activity and promoted by high-energy media.

Conclusions In summary, MII oocytes exhibit high heterogeneity in DSB repair, which is regulated by both metabolic factors and CDK1 activity. These results not only expand our understanding of oocyte DSB repair but also contribute to the modification of in vitro maturation medium for oocytes.

Keywords Oocytes, Double-strand breaks, RAD51, 53BP1, Break-induced replication, Theta-mediated end joining

*Correspondence:
Qin Zhang
zhangqinniuniu@163.com
Shen Yin
syin@qau.edu.cn
Xiang-Hong Ou
ouxianghong2003@163.com
Jun-Yu Ma
majy@gd2h.org.cn
[1] Guangzhou Key Laboratory of Metabolic Diseases and Reproductive Health, The Affiliated Guangdong Second Provincial General Hospital of Jinan University, Guangzhou, China
[2] Reproductive Medicine Center, The Affiliated Guangdong Second Provincial General Hospital of Jinan University, Guangzhou, China
[3] The Second School of Clinical Medicine, Southern Medical University, Guangzhou, China
[4] College of Life Sciences, Qingdao Agricultural University, Qingdao, China

Background

Eukaryotic nuclear DNA double-strand breaks (DSBs) are mainly repaired by the homology-directed repair (HDR) and nonhomologous end joining (NHEJ) pathways [1]. The competition between these DNA repair pathways mainly depends on the cell cycle phase and DNA end conditions [1, 2]. In the G1 phase, the DNA end resection of DSBs is inhibited by 53BP1 (TRP53BP1 in mouse or TP53BP1 in human), which promotes the ability of the KU protein-mediated NHEJ pathway to ligate double DSB ends [3]. However, in the S phase, the accumulation of 53BP1 on DSBs is antagonized by BRCA1, so that DSB ends can be resected, and the 3′ overhangs can bond with the strand exchange protein RAD51, which then mediates DSB repair via HDR [4]. During HDR repair of DSBs in the S and G2 phases, BRCA1 foci formation at DSB sites is promoted by the activity of cyclin-dependent kinase 1 (CDK1) [3, 5], which complexes with cyclin B 1 (CCNB1) and plays critical roles in the cell transition from the G2 phase to the mitosis phase [6]. The DNA binding affinity of RAD51 can also be activated by the CDK1/CCNB1 complex during the G2/M phase [7]. In addition to classical HDR and NHEJ, DSBs can also be repaired by alternative short homology-mediated DSB repair pathways, such as single-strand annealing, polymerase theta-mediated end joining (TMEJ) and break-induced replication (BIR) [1, 8, 9]. All these repair pathways form a decision tree for DSB repair, where cells can not only choose the pathway for DSB repair but also switch repair pathways during the DSB repair process [10]. Although these DSB repair mechanisms are flexible and well designed, DSBs can still be repaired erroneously or untimely, which will lead to de novo genome mutation, cell cycle delay, or even cell death. During sexual reproduction, the genome stability of germline cells needs to be maintained to suppress the accumulation of deleterious mutations in the gene pool [11]. Investigation of the DSB repair pathway in germline cells is essential for preventing the accumulation of deleterious mutations in germ cells and the germ cell loss caused by DNA damage. However, the DNA damage response, genome stability maintenance mechanism, and mutation features are remarkably diverse in different germline cells and should be studied separately [12, 13].

For adult females, fully grown germinal vesicle (GV)-stage oocytes need to extrude one set of homologous chromosomes before fertilization. This process is termed oocyte maturation, which starts with the resumption of meiosis in GV oocytes and ends at the metaphase II (MII) stage (Fig. 1). Generally, the segregation of homologous chromosomes during oocyte maturation can last for approximately 9 h in mice [14]

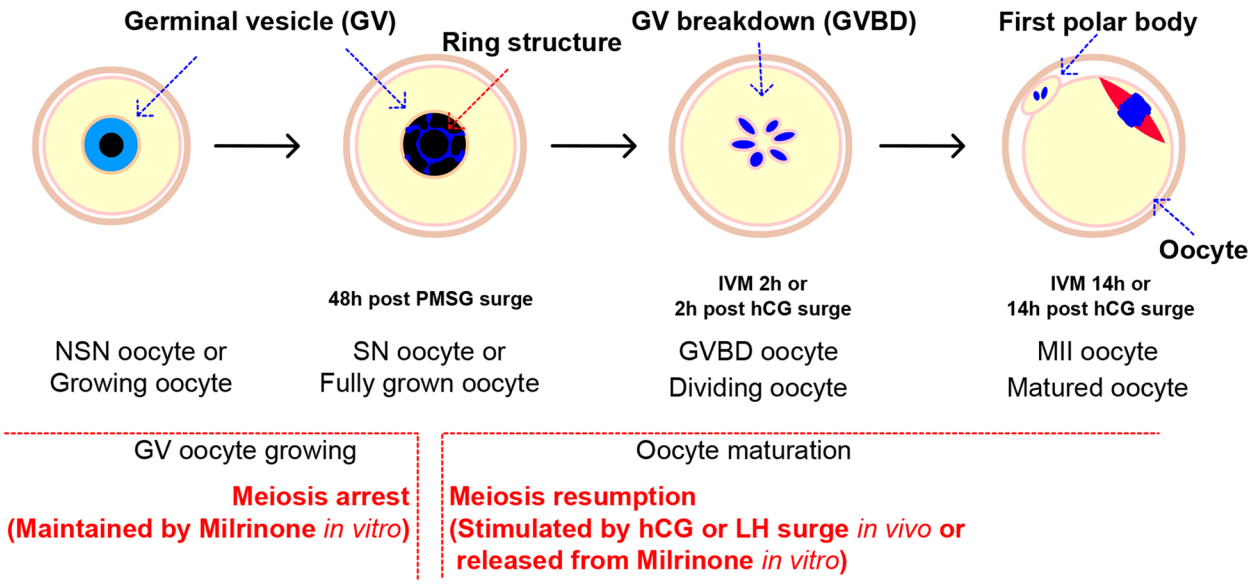

Fig. 1 The maturation process of mouse oocytes. In the growing oocytes, the chromatin is decondensed and DNA transcription is active. When the oocytes are fully-grown, the transcription is silenced and chromatin is condensed. At this time, a ring-like Hoechst positive structure surrounds the nucleolus (SN), so these oocytes are termed as SN oocytes, and correspondingly, the growing oocytes without SN are termed as Non-SN (NSN) oocytes. Both NSN and SN oocytes are meiosis arrested. At the in vivo condition, surge of endogenous luteinizing hormone (LH) or exogenous human chorionic gonadotropin (hCG) can initiate the meiosis resumption of SN oocytes. At the in vitro condition, the meiosis resumption of SN oocytes can occur automatically, and can be blocked by the Milrinone. Generally, 48 h after the injection of pregnant mare serum gonadotropin (PMSG) in mouse, the SN oocytes can be fully prepared for meiosis resumption. After meiosis resumption in vivo or in vitro, the germinal vesicle (GV) of oocytes will breakdown (GVBD). Then the first polar body (PB1) is extruded and oocyte is finally arrested at metaphase of the second meiosis (MII) stage, at which stage oocytes are matured for fertilization

or more than 20 h in humans [15], which strongly exceeds the division time required for second oocyte meiosis and somatic cell mitosis. For women with premature ovarian insufficiency or who are undergoing emergency cancer treatment, immature GV oocytes might be retrieved and matured in vitro to the MII stage and cryopreserved for fertility preservation [16]. In addition, during normal human assisted reproduction, immature GV and metaphase I (MI) oocytes can also be used when the number of retrieved MII oocytes is insufficient [17]. For these in vitro matured oocytes, specialized culture media are important for maintaining their developmental potential and genome stability. Recent studies have shown that DSBs can form in dividing oocyte chromosomes [14, 15], which might be caused by different factors, such as topological stress [18], or inherited from the GV stage [19, 20]. In dividing and MII oocytes, HDR and NHEJ have been reported to be responsible for DSB repair [21, 22]. However, little is known about whether there are other options for DSB repair in oocytes and how DSB repair is regulated. During oocyte maturation, CDK1 and CCNB1 are critical for oocyte GV breakdown (GVBD) [23] and aneuploidy prevention [24]; however, how DSB repair is regulated by CDK1 in oocytes has not been investigated.

In addition to intrinsic DSB repair pathways, exogenous factors can also regulate these DNA transactions. In vitro culture conditions are also critical factors affecting the DSB formation and repair in cells. In human embryonic stem cells, low pH and high reactive oxygen species caused by specific culture media can interfere with DSB repair [25, 26]. During human assisted reproduction, in vitro culture of gametes and early embryos is needed, whereas the in vitro maturation (IVM) medium for oocytes still needs improvement. However, whether there is a difference in genome stability between in vitro matured oocytes and in vivo matured oocytes and whether different culture media can affect oocyte DNA repair have not yet been analyzed. Therefore, in this study, we investigated DSB repair in maturating and matured oocytes, as well as the effects of culture medium on oocyte DSB repair.

Results

BIR-mediated repair of DSBs is suppressed in metaphase II oocytes

In our previous study, we found that DSBs in fully grown GV oocytes (also termed SN oocytes due to the ring-like Hoechst-positive structure surrounding the nucleolus, Fig. 1) can be repaired by the BIR mechanism (Fig. 2A) [27]. To analyze the features of DSB repair in the dividing oocytes, treatment with 10 μM Bleomycin for 1 h was used for DSB induction in the oocytes at different IVM stages. The IVM stages included IVM 2 h, when the oocytes had undergone GVBD; IVM 5 h, when the oocytes had developed at the premetaphase I stage; IVM 9 h, when the oocytes had developed to anaphase I to the telophase I stage; and IVM 12 h and 14 h, when the oocytes had extruded their first polar bodies (PB1). After 6 h of recovery from Bleomycin, BIR-mediated repair of DSBs was detected by an EdU click reaction. All these oocyte manipulations and cultivations were performed in M2 media. As a result, we found that BIR repair of DSBs could be observed at all maturation stages of the dividing oocytes. However, the percentage of oocytes with strong EdU signals was greatest at the IVM 2 h stage (97.0%) and decreased gradually to 46.8% at the IVM 14 h stage ($p < 0.01$, Tukey HSD test, Fig. 2A and B), indicating that the BIR repair of DSBs was suppressed as the oocyte maturation. In addition, we compared the EdU signals between oocyte and PB1 in the IVM 14 h oocytes, and the result showed that BIR was suppressed in PB1 (0% of PB1 had strong EdU signals vs 60% of oocytes had strong EdU signals, $p < 0.01$ according to Fisher's exact test; Fig. 2C). These results indicated that the BIR participated DSB repair in dividing oocytes and was suppressed at the MII stage. In addition, DSB repair by BIR was strongly inhibited in PB1 of the MII oocytes.

To understand the molecular mechanism of BIR-mediated DSB repair in dividing oocytes, we treated IVM 2 h oocytes with Bractoppin which inhibits the critical HDR repair protein BRCA1, or Aphidicolin which inhibits DNA polymerase α and δ. For Bractoppin treatment, the GV oocytes were firstly blocked from GVBD by Milrinone. After treatment with Bractoppin (100 μM) for 3 h, these oocytes were released from Milrinone, and IVM in M2 medium for 2 h. Then, the oocytes were inducted with DSBs by Bleomycin (10 μM/1 h) and released from Bleomycin for more than 6 h. After EdU click reaction, we found the percentage of oocytes with strong EdU signals decreased from 94.1% in the control group to 55.9% in the Bractoppin treatment group ($p < 0.01$, Tukey HSD test, Fig. 2D). For the Aphidicolin treatment, GV oocytes were also firstly blocked from GVBD by Milrinone. After treatment with 0 μM, 3 μM, or 10 μM Aphidicolin for 3 or 10 h, the GV stage oocytes were released from Milrinone and IVM in M2 medium. After 2 h of IVM, oocytes were induced with DSBs by Bleomycin (10 μM/1 h) and released from Bleomycin for more than 6 h (Fig. 2E). After EdU click reaction, we found that the percentage of oocytes with strong EdU signals decreased significantly (from 92.6% in the 0 μM/3 h group to 62.5% in the 3 μM/3 h group, $p < 0.01$; and to 48.4% in the 10 μM/3 h group, $p < 0.01$; Fisher's exact test). Compared with those of the 10 μM/3 h Aphidicolin treated oocytes, when the oocytes were treated with 10 μM Aphidicolin for 10 h at

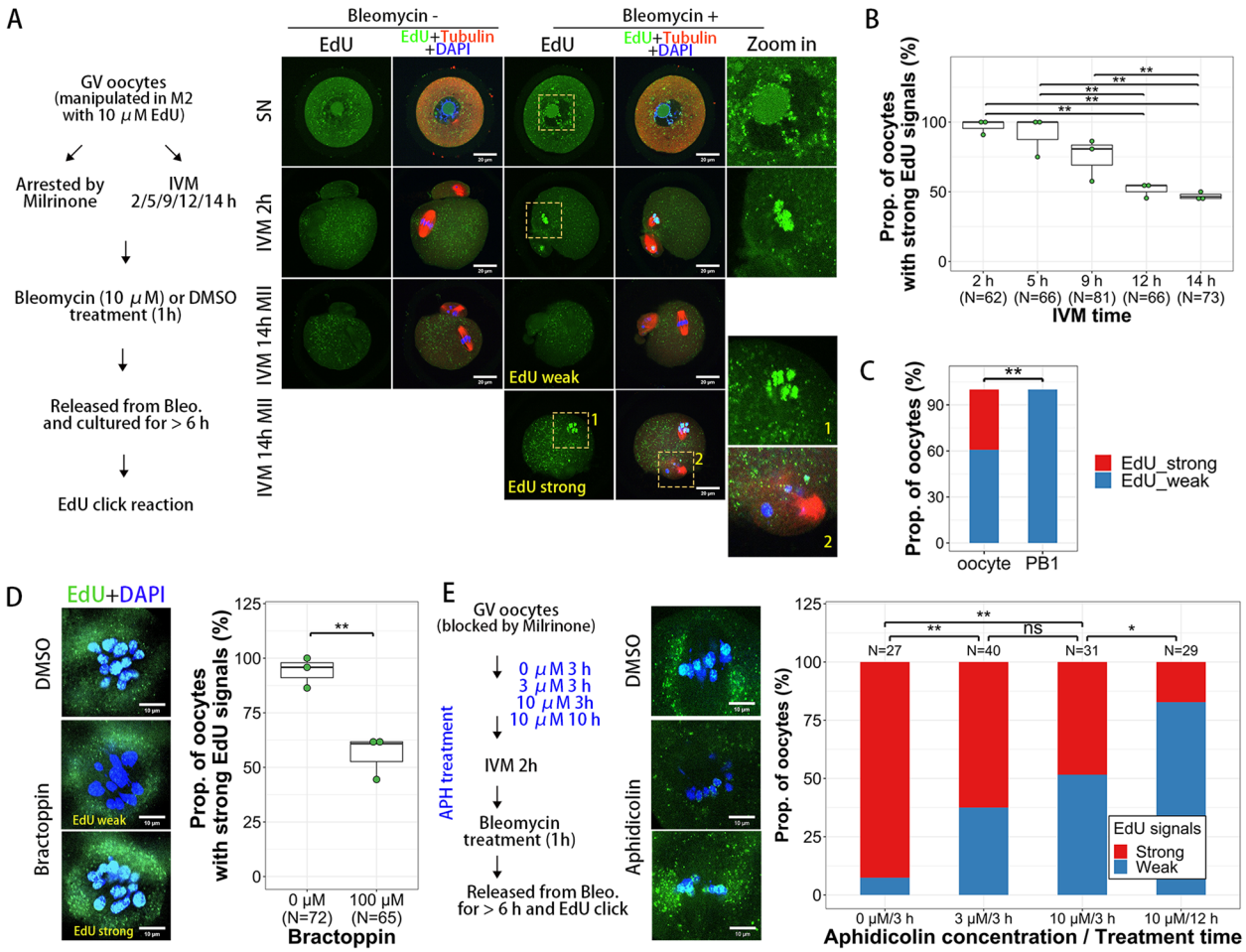

Fig. 2 Break-induced replication is suppressed in metaphase II oocytes. **A** DSB-induced DNA synthesis in oocytes at different developmental stages. Newly synthesized DNA was labeled by the EdU click reaction. Scale bar, 20 μm; GV, germinal vesicle; SN, fully grown oocytes with a Hoechst-positive ring-like structure surrounding the nucleolus; IVM, in vitro maturation. Dashed box with number 1, oocyte chromosomes; dashed box with number 2, the first polar body (PB1) chromosomes. **B** The proportions of DSB oocytes with strong EdU signals during oocyte IVM (statistics performed by Tukey HSD test). Oocytes with extruded PB1 were selected for induction of DSBs in the IVM 12 h and 14 h groups. **C** No strong EdU signal is detected in PB1 of the IVM 14 h DSB oocytes ($N = 73$; statistics performed by Fisher's exact test; scale bar, 10 μm). **D** Break-induced replication in IVM 2 h DSB oocytes was suppressed by the BRCA1 inhibitor Bractoppin (statistics performed by Tukey HSD test). **E** Break-induced replication in IVM 2 h DSB oocytes was suppressed by the DNA polymerase inhibitor Aphidicolin (APH). Statistics performed by Fisher's exact test. Scale bar, 10 μm. GV oocytes, which were maintained in GV state by milrinone, were firstly treated by APH with different concentrations and different times. Then oocytes were released from milrinone and IVM for 2 h. The break-induced replication was analyzed in these IVM 2 h oocytes. Significance markers: *, $p < 0.05$; **, $p < 0.01$; ns, $p > 0.05$. Repeat number and sample size are indicated by the number of dots in the dot plots

the GV stage, the percentage of oocytes with strong EdU signals further decreased from 48.4% in the 10 μM/3 h group to 17.2% in the 10 μM/10 h group ($p < 0.05$, Fisher's exact test, Fig. 2E). These results indicating that HDR and DNA polymerase α or δ participated in the repair of DSBs in dividing oocytes.

BIR suppression is strengthened in MII oocytes which are matured in vivo or by DMEM

For mammalian oocytes, their energy materials such as glucose and pyruvate are mostly supplied by the surrounding cumulus cells [28]. Cumulus cells can also control the DSB sensitivity in oocytes [29]. For mouse, oocyte could be super-ovulated by injection of pregnant mare serum gonadotropin (PMSG) and human chorionic gonadotropin (hCG) (Fig. 1) [30]. When PMSG was injected for 48 h, the oocytes could be synchronized to the fully grown stage and be fully prepared for ovulation. Then, when hCG was injected into mouse, the oocytes would resume meiosis immediately. To analyze whether the BIR repair of DSBs is affected by cumulus cells and which factors participate in the regulation of

oocyte DSB repair, we collected two groups of in vivo oocytes and four groups of IVM oocytes. The in vivo oocytes were collected from mice that were injected with hCG for 2 h (hCG 2 h, corresponding to IVM 2 h oocytes) or 14 h (hCG 14 h, corresponding to IVM 14 h oocytes). The four groups of IVM oocytes includes (1) DMEM-cultured IVM 14 h oocytes originating from the cumulus-enclosed oocytes (CEOs), which were collected at 48 h post PMSG injection (PMSG 48 h CEO DMEM IVM 14 h); (2) DMEM-cultured denuded oocytes (DO) from the PMSG 48 h CEOs (PMSG 48 h DO DMEM IVM 14 h); (3) DMEM-cultured DOs collected from mice without PMSG injection (DO DMEM IVM 14 h); and (4) M2-cultured DOs collected from mice without PMSG injection (DO M2 IVM 14 h). After treating these oocytes with Bleomycin (10 μM/1 h) and released from Bleomycin for more than 6 h, strong EdU signals could only be found in the hCG 2 h oocytes (Fig. 3A), which is comparable to what was observed in M2 medium based IVM 2 h oocytes (Fig. 2A). However, no strong EdU signal was detected in oocytes from the PMSG 48 h CEO DMEM IVM 14 h, PMSG 48 h DO DMEM IVM 14 h, or DO DMEM IVM 14 h oocytes (Fig. 3A), which was significantly less than that in M2 based IVM 14 h oocytes ($p < 0.01$, Fisher's exact test, Fig. 3A). These results indicated that the DSB repair choice of MII oocytes might be affected by the metabolic micro-environment of the medium.

As different culture media induced the different DSB repair features in these MII oocytes, we compared the recipes of DMEM and M2 media. We found that M2 medium has a lower content of glucose (5.56 mM in M2 vs 25 mM in DMEM) and sodium pyruvate (0.33 mM in M2 vs 1 mM in DMEM) and a different serum component (4.0 g/L BSA in M2 vs 10% FBS in DMEM) and has no supplementation with essential or nonessential amino acids. To determine which factors in culture medium can affect DSB repair in oocytes, the M2 medium was supplemented with glucose (0.3 mg of glucose per 100 μL of M2, M2 + Gl), sodium pyruvate (144 μg of sodium pyruvate per 100 μL of M2, M2 + Py), FBS (10%, M2 + FBS), glucose + sodium pyruvate (M2 + G.P.), glucose + sodium pyruvate + FBS (M2 + G.P.F.), and glucose + sodium pyruvate + FBS + essential/nonessential amino acids

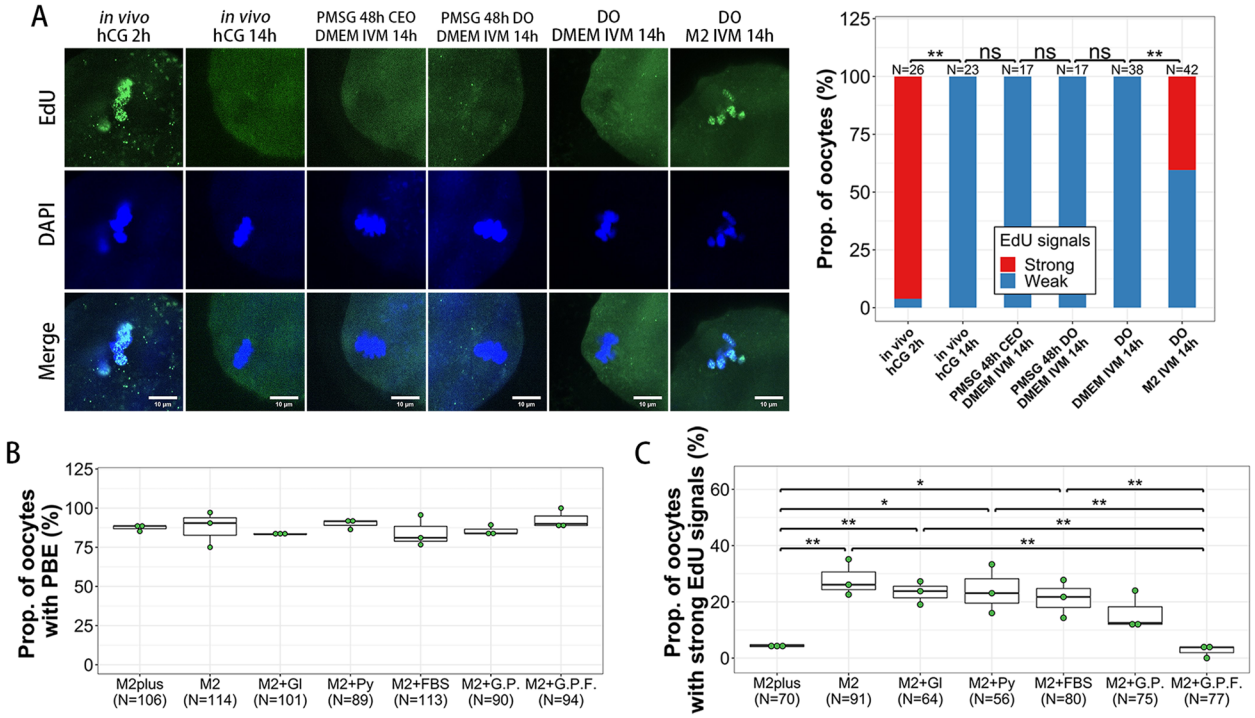

Fig. 3 Break-induced replication in MII oocytes is regulated by the culture medium. **A** Break-induced replication in in vivo oocytes (2 h or 14 h after hCG injection), DMEM-cultured cumulus-enclosed oocytes (CEOs, IVM 14 h), DMEM-cultured denuded oocytes (DOs, IVM 14 h), and M2-cultured DOs (IVM 14 h). EdU strong signals could be detected in in vivo hCG 2 h DSB oocytes and in M2 cultured IVM 2 h DSB DO oocytes. Statistics performed by Fisher's exact test. **B** IVM medium had no obvious effect on the polar body extrusion (PBE) rate of oocytes. Statistics performed by Tukey HSD test. **C** Break-induced replication is suppressed in M2 + G.P.F. and M2plus group oocytes. Statistics performed by Tukey HSD test. Gl, glucose; Py, sodium pyruvate; G.P., glucose + sodium pyruvate; G.P.F., glucose + sodium pyruvate + FBS; M2plus, M2 + glucose + sodium pyruvate + FBS + essential/nonessential amino acids. Scale bar, 10 μm. Significance markers: *, $p < 0.05$; **, $p < 0.01$; ns, $p > 0.05$. Repeat number and sample size are indicated by the number of dots in the dot plots

(1 × essential/nonessential amino acids, M2plus) separately, and these modified M2 media were used to culture oocytes and detect the BIR repair of DSBs. As a result, we found that there was no obvious difference in the polar body extrusion rate among these media (Tukey HSD test, Fig. 3B). However, when the IVM 14 h oocytes were treated with Bleomycin (10 μM/1 h) and released from Bleomycin for more than 6 h, the frequency of DSB oocytes with strong EdU signals was significantly decreased in M2 + G.P.F. (2.6%, $p < 0.01$) and M2plus (4.4%, $p < 0.01$, Tukey HSD test) groups, compared with that in the oocytes matured in M2 (27.9%) (Fig. 3C). In addition, M2plus and M2 + G.P.F. cultured MII oocytes had lower strong EdU signal rates than that in M2 + Gl (23.4%, $p < 0.05$ for M2plus group and $p < 0.01$ for M2 + G.P.F. group), M2 + Py (24.1%, 23.4%, $p < 0.05$ for M2plus group and $p < 0.01$ for M2 + G.P.F. group), and M2 + FBS (21.3%, 23.4%, $p < 0.05$ for M2plus group and $p < 0.01$ for M2 + G.P.F. group) cultured ones (Tukey HSD test, Fig. 3C). These results indicated that BIR suppression in DMEM is caused by multiple metabolic factors.

RAD51-mediated homology-directed repair but not 53BP1-mediated NHEJ in MII oocytes is suppressed by DMEM

To study whether DMEM culture affects other DSB repair pathways, we analyzed the focus formation of the HDR protein RAD51 and the NHEJ protein 53BP1 in DSB oocytes. By microinjection of *GFP-RAD51* cRNAs into the Milrinone-blocked SN oocytes for 3 h and treated oocytes by Bleomycin (10 μM) for 1 h, we found that GFP-RAD51 foci could be found in DSB SN oocytes cultured by M2 medium (Fig. 4A), which is consistent with our previous results [14, 27]. To analyze the effects of different media on RAD51 foci formation in GVBD oocytes, *GFP-RAD51* cRNAs were injected into Milrinone-blocked GV oocytes for 2 h, then oocytes were released from Milrinone and cultured in M2 or DMEM for 2 h. After treating with 10 μM of Bleomycin for 1 h, GFP-RAD51 foci could be found in all the DSB oocytes cultured by M2 or DMEM (Fig. 4B), indicating that RAD51 is important for DSB repair in dividing oocytes, which is similar to the findings in somatic cells [31]. When IVM 2 h oocytes cultured by M2 or DMEM were inducted with DSBs by Bleomycin (10 μM/1 h), and released from Bleomycin for 1 h, the antibody labeled RAD51 foci could be found associating with the newly synthesized DNA marked by EdU (Fig. 4C). When oocytes were matured to MII stage by M2 or DMEM, the formation of GFP-RAD51 focus after DSB induction was also different. For the M2 cultured oocytes, after release from Bleomycin treatment for 1 h, 3 h, and 6 h, the percentages of DSB oocytes with GFP- RAD51 foci were 27.6%, 50.9%, and 50.0%, respectively; however, for the DMEM-cultured oocytes, these percentages were 0%, 0%, and 18.2%, respectively, which were significantly lower than those formed in the M2-cultured ones ($p < 0.01$ for oocytes released from Bleomycin for 3 h and $p < 0.05$ for the other two groups, Fisher's exact test, Fig. 4D), indicating that the RAD51-mediated HDR pathway in MII oocytes was suppressed by DMEM.

As RAD51-mediated strand exchange is one of the different factors that induces BIR [9], we analyzed the correlation of GFP-RAD51 foci with the EdU signal in M2-cultured DSB MII oocytes, which had been released from Bleomycin treatment (10 μM/1 h) for 3 h. As a result, in the 18 EdU signal-negative oocytes, GFP-RAD51 foci were also negative, and in the 36 EdU signal-positive oocytes, GFP-RAD51 foci were negative in 10 oocytes and positive in 26 oocytes ($p < 0.01$, Fisher's exact test, Fig. 4E), indicating that RAD51 protein was associated with BIR repair in MII oocytes; however, it was possible that not all BIR events in DSB MII oocytes were directly induced by RAD51.

Then, we analyzed the effects of IVM medium on 53BP1 foci formation. After microinjection of *GFP-53BP1* mRNA into oocytes which were cultured by M2 for different time, these oocytes were then treated with Bleomycin (10 μM/1 h) and released from Bleomycin for 0.5 h. As a result, we found that GFP-53BP1 foci were not detected in GV oocytes or IVM 2 h GVBD oocytes but could be detected in IVM 14 h MII oocytes (0, 0, and 9.7 foci in average respectively, $p < 0.01$, Kramer-Nemenyi test, Fig. 4F), indicating that NHEJ-mediated repair of DSBs was promoted in MII stage oocytes. Then, we counted the number of GFP-53BP1 foci in M2- and DMEM-cultured MII oocytes which were treated with Bleomycin (10 μM/1 h) and released from Bleomycin for 0.5 h, 1 h, or 5 h. For DMEM cultured oocytes, compared with those in the 1-h group of oocytes, the number of GFP-53BP1 foci was significantly less in the 5-h group of DMEM-treated oocytes (11.9 foci in average vs 3.8 foci, $p < 0.05$, Kramer-Nemenyi test). For M2 cultured oocytes, compared with 1-h group oocytes, the number of GFP-53BP1 foci was also significantly less in the 5-h group oocytes (12.4 foci in average vs 2.3 foci, $p < 0.01$, Kramer-Nemenyi test, Fig. 4G). At all three time points, there was no significant difference in the number of GFP-53BP1 foci between M2- and DMEM-cultured oocytes (Kramer-Nemenyi test, Fig. 4G), indicating that DMEM could not suppress or promote NHEJ in MII-stage oocytes.

BIR in MII oocytes is regulated by CDK1

Because the activity of the CDK1/CCNB1 complex is critical for both oocyte maturation and DSB repair [7, 23, 24], we analyzed whether CDK1 affects DSB repair

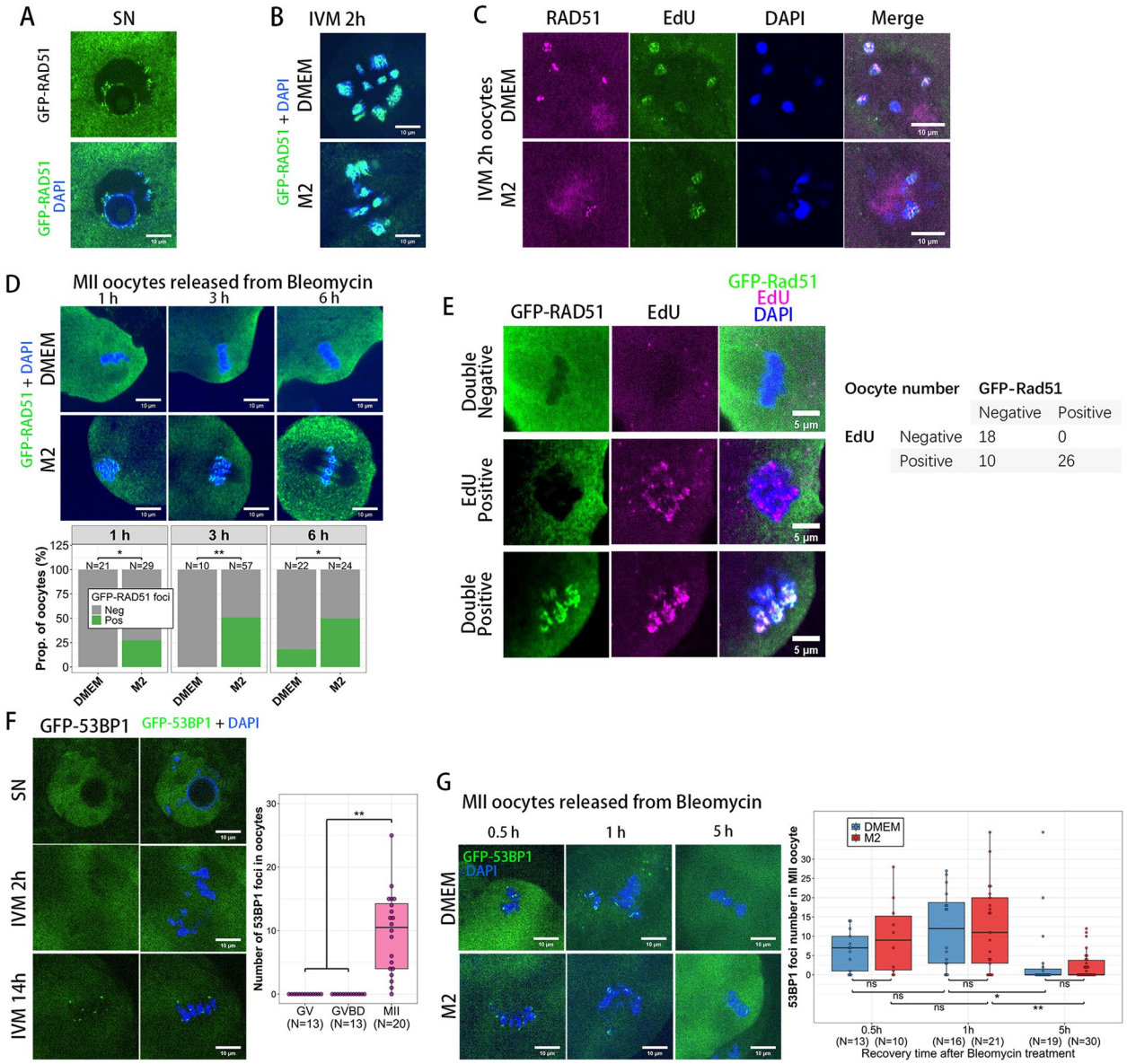

Fig. 4 RAD51-mediated homology-directed repair but not nonhomologous end joining is suppressed in MII oocytes. **A** GFP-RAD51 foci can be found in Bleomycin treated SN oocytes. **B** In IVM 2 h oocytes, GFP-RAD51 foci formed in both DMEM and M2 cultured DSB oocytes. **C** RAD51 foci associated with EdU signals in both DMEM and M2 cultured DSB IVM 2 h oocytes. **D** The formation of GFP-RAD51 foci was suppressed in MII oocytes which were matured in DMEM. Statistics performed by Fisher's exact test. **E** GFP-RAD51 foci formation correlated with break-induced replication (BIR). BIRs are marked by EdU signals at chromosome regions. **F** The DSB caused GFP-53BP1 foci formation was inhibited in GV and IVM 2 h oocytes but activated in IVM 14 h MII oocytes. **G** There was no significant difference in the number of GFP-53BP1 foci between M2- and DMEM-cultured oocytes after DSB induction. Scale bar, 5 μm for **E** and 10 μm for others. Significance markers: *, $p < 0.05$; **, $p < 0.01$; ns, $p > 0.05$. Statistics performed by Kramer-Nemenyi test. Repeat number and sample size are indicated by the number of dots in the dot plots

in oocytes during IVM and whether there was a difference in CDK1 protein levels between M2- and DMEM-cultured oocytes. After treating the Milrinone blocked GV oocytes with the CDK1 inhibitor RO-3306 [32] or DMSO for 3 h, these oocytes were treated with Bleomycin (10 μM/1 h) and released from Bleomycin for more than 6 h. As a result, in these oocytes, the volumes of DSBs induced γH2A.X signals had no obvious difference between DMSO and RO-3306 treated groups; however, the number of EdU foci decreased in these RO-3306 treated DSB oocytes (the average number of foci was 45.9 in RO-3306-treated oocytes vs 102.7 in the DMSO control group, $p < 0.05$, Kramer-Nemenyi test, Fig. 5A), indicating that CDK1 participated in BIR regulation in

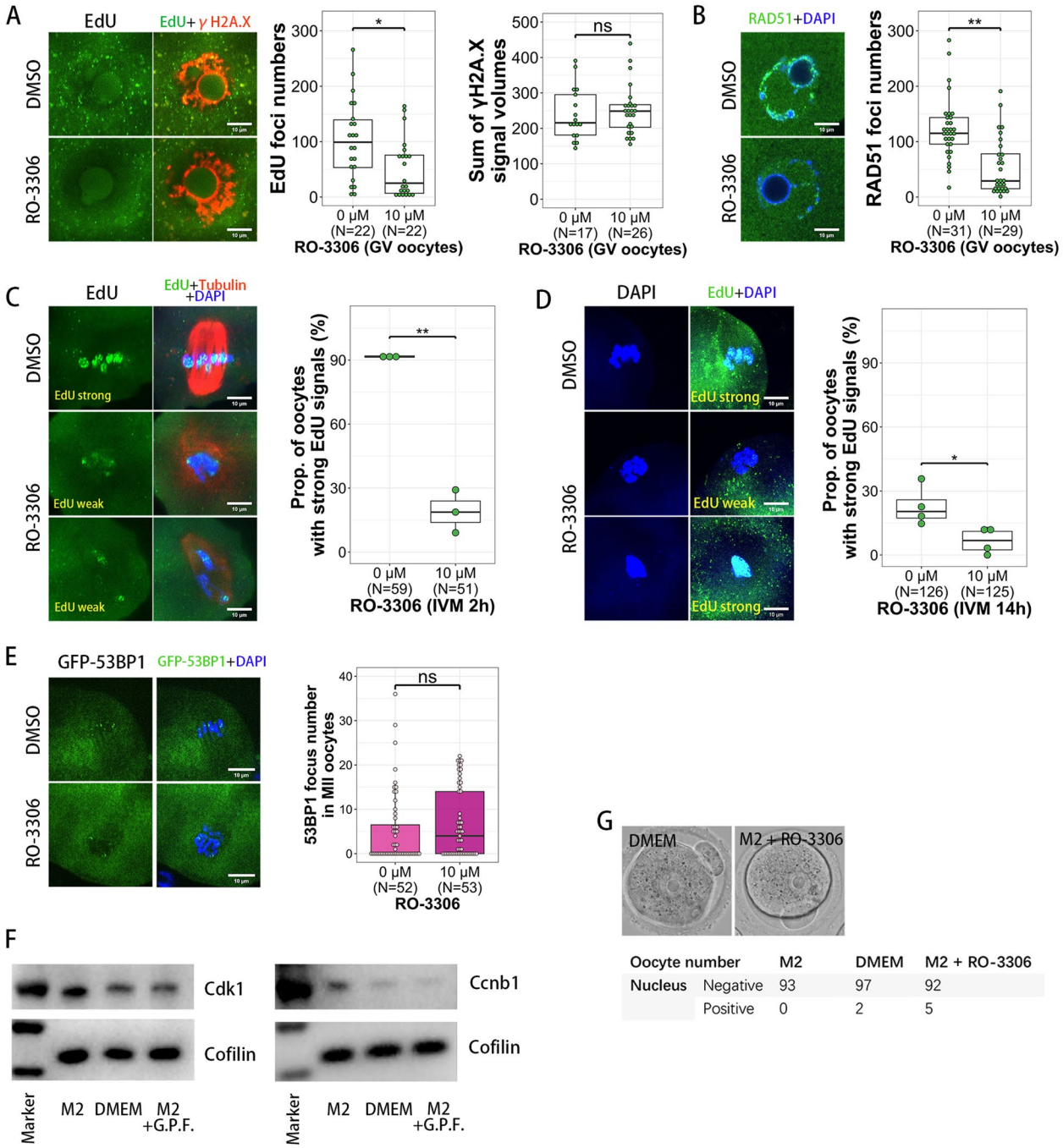

Oocyte number		M2	DMEM	M2 + RO-3306
Nucleus	Negative	93	97	92
	Positive	0	2	5

Fig. 5 CDK1 regulates break-induced replication and RAD51-mediated homology-directed repair in MII oocytes. **A** The CDK1 inhibitor RO-3306 suppressed the number of EdU foci in SN DSB oocytes but did not affect the total γH2A.X volume. Statistics performed by Kramer-Nemenyi test. **B** CDK1 inhibitor RO-3306 suppressed the RAD51 foci formation in DSB SN oocytes. Statistics performed by Kramer-Nemenyi test. **C**, **D** RO-3306 decreased the proportion of oocytes with strong EdU signals when the DSBs were introduced at IVM 2 h **C** or IVM 14 h **D**. Statistics performed by Tukey HSD test. **E**(D) RO-3306 had no significant effect on the number of GFP-53BP1 foci in DSB MII oocytes. The oocytes were treated with 10 μM of Bleomycin for 1 h and released from Bleomycin for 1 h. Statistics performed by Kramer-Nemenyi test. **F** Compared with those in oocytes matured in M2 medium, the protein levels of CDK1 and CCNB1 in oocytes matured in DMEM or M2 + glucose + pyruvate + FBS (M2 + G.P.F.) medium decreased. Cofilin was used as an internal reference protein. **G** Pronucleus-like nuclei can be found in DMEM-matured oocytes and RO-3306-treated MII oocytes. Scale bar, 10 μm. Significance markers: *, $p < 0.05$; **, $p < 0.01$; ns, $p > 0.05$. Repeat number and sample size are indicated by the number of dots in the dot plots

GV oocytes. Using the same method, we also analyzed the effects of RO-3306 on the RAD51 foci formation in DSB GV oocytes. As a result, we found that RO-3306 also suppressed the RAD51 foci formation in DSB GV oocytes (in DMSO control oocytes, the average number of RAD51 foci was 123.3; in RO-3306-treated oocytes, the average number is 54.7; $p < 0.01$, Kramer-Nemenyi test, Fig. 5B). Similar to GV oocytes, after treating IVM 2 h and IVM 14 h oocytes with Bleomycin (10 μM/1 h) and released from Bleomycin for more than 6 h, the percentage of oocytes with strong EdU signals also significantly decreased in RO-3306 treated DSB oocytes (for IVM 2 h oocytes, 91.6% in the control group vs 19.0% in the RO-3306 group, $p < 0.01$; for IVM 14 h oocytes, 24.3% in the control group vs 9.0% in the RO-3306 group, $p < 0.05$; Tukey HSD test, Fig. 5C and D). Next, we detected whether RO-3306 could affect 53BP1 formation in M2-cultured DSB MII oocytes. As a result, there RO-3306 had no obvious effect on the GFP-53BP1 foci formation in DSB MII oocytes (an average of 5.1 GFP-53BP1 foci formed in the control DSB MII oocytes vs 6.8 foci formed in the RO-3306-treated ones, $p > 0.05$, Kramer-Nemenyi test; Fig. 5E). These results indicated that the HDR pathways but not NHEJ were regulated by the activity of CDK1 in oocytes.

To study whether the suppression of BIR- and RAD51-mediated HDR was associated with CCNB1/CDK1 protein levels in DMEM or the M2 + G.P.F. medium cultured oocytes, we detected the CDK1 and CCNB1 protein levels in MII oocytes that were matured in vitro in M2, DMEM or M2 + G.P.F. medium. Compared with those in MII oocytes matured in M2, the protein levels of both CDK1 and CCNB1 were decreased in oocytes matured in DMEM and M2 + G.P.F. medium (Fig. 5F). It has been reported that when CDK1 is suppressed, the metaphase chromosomes in MII oocytes can break through MII arrest and transform into the nucleus [33]. Indeed, when oocytes were matured in DMEM for 24 h or matured in M2 medium for 12 h and treated with RO-3306 for 12 h, a pronucleus-like single nucleus could be found in a small number of oocytes (2 in 99 DMEM-cultured oocytes and 5 in 97 RO-3306-treated M2 cultured oocytes), but no nucleus was found in oocytes which were matured in M2 medium for 24 h (Fig. 5G). Although there was no significant difference in the proportion of oocytes forming new nucleus among the groups, the increase of the number of oocytes with nucleus suggested that the activity of CDK1 in the DMEM-cultured and RO-3306-treated oocytes had indeed been weakened.

Then, the exogenous cRNAs expressing *CCNB1-mVenus* and *CDK1-mCherry* were used to further confirm the functions of CCNB1/CDK1 on oocyte DSB repair. Firstly, the cRNAs of *EGFP*, *CCNB1-mVenus*, *CDK1-mCherry*, and *CCNB1-mVenus* mixed with *CDK1-mCherry* were micro-injected into the GV oocytes which had been blocked by Milrinone. The fluorescent protein signals could be detected 3 h post cRNA micro-injection. And after 8 h, comparing to the oocytes injected with EGFP cRNAs (none of which had GVBD, $N = 26$), there were 80.0% ($N = 40$), 39.4% ($N = 33$), and 100% ($N = 23$) of oocytes injected with *CCNB1-mVenus*, *CDK1-mCherry*, and *CCNB1-mVenus* + *CDK1-mCherry* cRNAs, had GVBD respectively ($p < 0.01$, Fisher's exact test, Fig. 6A). Secondly, the cRNAs of *EGFP* and *CCNB1-mVenus* mixed with *CDK1-mCherry* were micro-injected into the MII oocytes which were in vitro matured by M2 + G.P.F. medium. After waiting for 3 h for the expression of exogenous cRNAs, the oocytes were treated with Bleomycin (10 μM/1 h) and released from Bleomycin for 6 h. Then, the newly synthesized DNA were detected by EdU click reaction. As a result, there were 15.4% of oocytes ($N = 26$) had strong EdU signals in for the *EGFP* injected oocytes; whereas there were 85.4% of oocytes ($N = 48$) had strong EdU signals for the *CCNB1-mVenus* + *CDK1-mCherry* injected oocytes ($p < 0.01$, Fisher's exact test, Fig. 6B), indicating that over-expression of CCNB1 and CDK1 could promote the BIR repair of DSB in MII oocytes.

TMEJ is promoted in MII oocytes by DMEM cultivation or CDK1 inhibition

It had been reported that POLQ-mediated TMEJ repairs DSBs in somatic cells at the mitotic stage [34]. Therefore, we analyzed whether TMEJ repairs DSBs in these MII oocytes. After DSB induction by Bleomycin (10 μM/1 h) and 1 h release from Bleomycin, the POLQ foci were detected in 40.0% of the DMEM-cultured MII oocytes but not in the M2-cultured MII oocytes ($p < 0.01$, Fisher's exact test, Fig. 7A), indicating that TMEJ-mediated DSB repair might not be used by all of the DMEM-cultured MII oocytes and that the TMEJ in MII oocytes was inhibited by M2 medium. Then, we analyzed whether the TMEJ pathway is associated with CDK1 activity. For the oocytes that matured in M2 + G.P.F. medium for 16 h, and the oocytes matured in M2 for 12 h and treated with RO-3306 for 4 h, after Bleomycin treating and releasing, the POLQ foci were detected in 50.0% and 35.0% of these oocytes, respectively. However, no POLQ foci were found in these DSB MII oocytes which had been matured in M2 medium for 16 h and inducted with DSBs ($p < 0.01$, Fisher's exact test, Fig. 7B). These results indicated that TMEJ participated in DSB repair in MII oocytes and was also regulated by CDK1.

Discussion

In the mitosis stage of somatic cells, DSB repair is suppressed to prevent telomere fusion [35]. In this study, the DSB repair in dividing oocytes were analyzed. Our

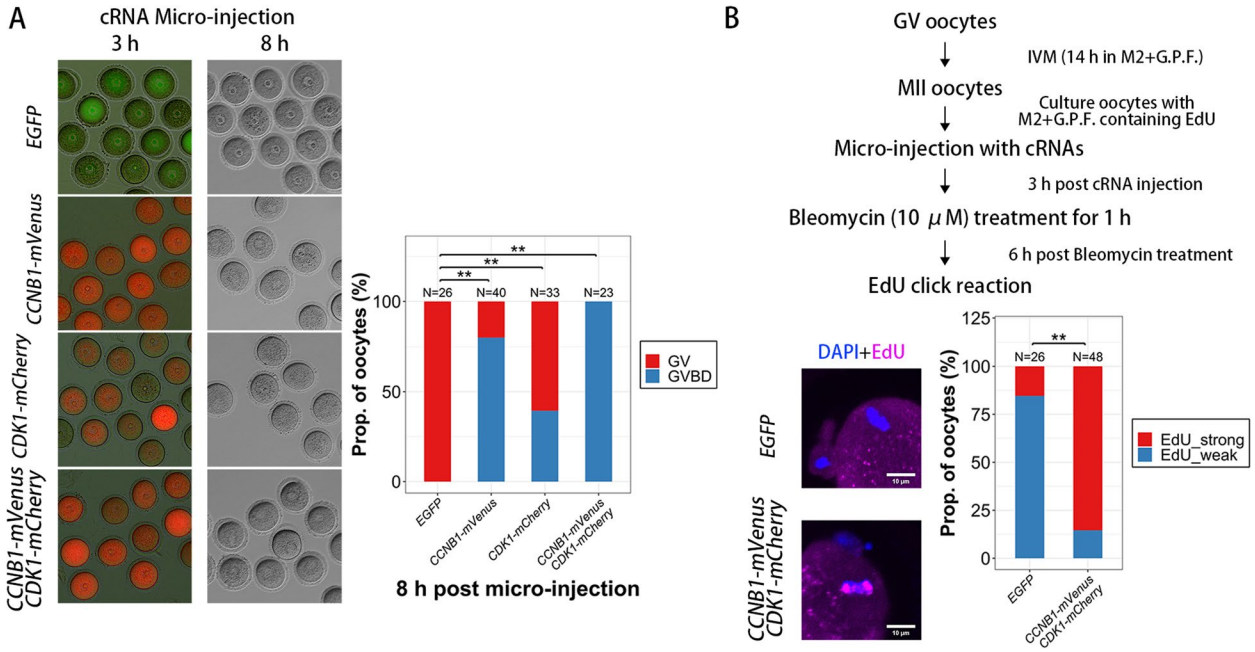

Fig. 6 Over-expression of CCNB1 and CDK1 promote break-induced replication in MII oocytes. **A** Over-expression of *CCNB1-mVenus*, *CDK1-mCherry* or *CCNB1-mVenus* mixed with *CDK1-mCherry* in GV oocytes could rescue the Milrinone induced GV arrest. The fluorescence signal could be detected 3 h after cRNA injection. The GVBD rates were recorded 8 h after cRNA micro-injection. Statistics performed by Fisher's exact test. **B** Over-expression of *CCNB1-mVenus* mixed with *CDK1-mCherry* promoted the break-induced replication in the MII oocytes which were matured in M2 + glucose + pyruvate + FBS (M2 + G.P.F.) medium. Statistics performed by Fisher's exact test. Scale bar, 10 μm. *EGFP* cRNAs were used as control. Significance markers: **, $p < 0.01$

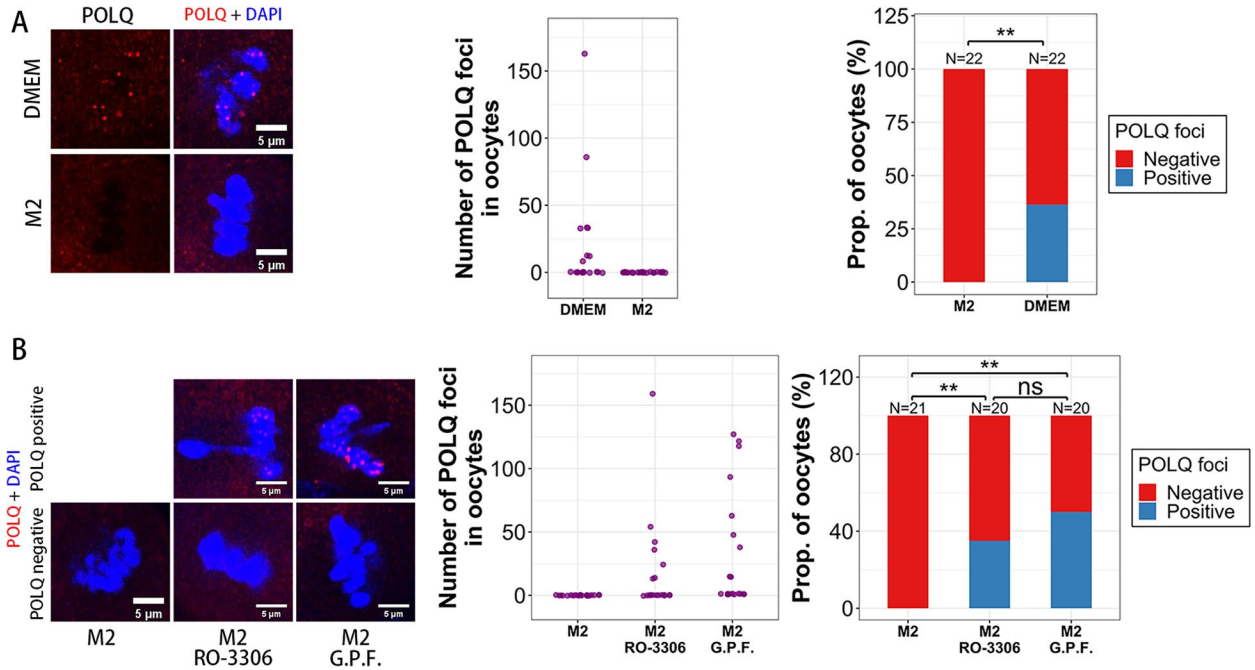

Fig. 7 CDK1 regulates polymerase theta-mediated end joining in MII oocytes. **A** POLQ foci can be found in DMEM-cultured MII oocytes but not in M2-cultured oocytes. Statistics performed by Fisher's exact test. **B** POLQ focus formation in MII oocytes can be promoted by adding the CDK1 inhibitor RO-3306 or glucose + pyruvate + FBS (G.P.F.) to M2 media. Statistics performed by Fisher's exact test. Scale bar, 5 μm. Significance markers: **, $p < 0.01$; ns, $p > 0.05$. Repeat number and sample size are indicated by the number of dots in the dot plots

results indicate that at least four options are available for repairing DSBs in MII oocytes, including RAD51-mediated HDR, NHEJ, BIR, and TMEJ, in which HDR, BIR, and TMEJ are regulated by Cdk1 activity and the oocyte culture media. NHEJ repair is inhibited in GV and GVBD (IVM 2 h) oocytes but is slightly activated in MII oocytes. In contrast, BIR- and RAD51-mediated HDR repair are highly activated in the GVBD stage oocytes but are suppressed in the MII stage oocytes. TMEJ repair can also be detected in the MII-stage oocytes, but it occurs only in a small proportion of oocytes that are matured in DMEM or M2 + G.P.F. medium. Our data showed that there were some oocytes whose DSBs could neither be repaired by BIR and RAD51-mediated HDR nor repaired by TMEJ. Considering that 53BP1 foci were vastly dispersed and were present in small numbers in DSB MII oocytes, it could be inferred that DSB repair was suppressed in some MII oocytes. The incomplete inhibition of DSB repair in MII oocytes could also indicate that there is inherent heterogeneity of DSB repair in these oocytes.

For mammalian early embryo development, the materials supporting the first few cell divisions are provided by the oocytes [36]. The DNA replication stress and DSB responses in early embryos are associated with the chromatin state and the materials carried by oocytes. It has been reported that maternal deletion of CHK1, would stabilize CDC25A and activate CDK1, causing the premature mitotic entry in about half of early embryos [37]. On one hand, this data indicates the regulation of CDK1 in oocyte and embryo are important; on the other hand, the heterogeneity of early embryos response to CHK1 deletion was manifested. As the early embryos are also cultured in artificially prepared culture medium like KSOM, which might also generate heterogeneity in embryos, just like the DSB repair heterogeneity in MII oocytes. Therefore, it should be paid attention to that whether the heterogeneity of the in vitro cultured embryos also exist in in vivo embryos or was the generation of heterogeneity related to the embryo cultivation conditions. It has been reported that DSBs can be generated by different mechanisms in oocytes and embryos [14, 15, 19, 38–41]. If it can be proven that metabolites have an impact on DNA response proteins, the different media used for gamete and embryo manipulation and cultivation during human assisted reproduction may affect the DSB repair in these cells and further affect the clinical outcomes.

In human preimplantation embryos, faster or earlier cleaving embryos generally have greater blastocyst morphological quality and greater implantation and birth rates [42, 43]. It has been reported that fast-cleaving zygotes have higher glucose consumption rates at the blastocyst stage, and the corresponding blastocysts have a lower rate of aneuploidy [44]. In addition, replication stress-generated DSBs in zygotes can persist into the G2 phase and lead to aneuploidy in embryos [45]. All these data indicated that DSB burden and delayed cell cycle might cause mitotic aneuploidy in preimplantation embryos. Although mitotic aneuploidy might be a universal phenomenon in human embryos and aneuploidy cells could be filtered out in the inner cell mass which carries cells that will develop into human individual [46], high rate of mitotic aneuploidy in embryos is absolutely harmful and would increase the risk of miscarriage and specific human diseases [47, 48]. In this study, CDK1 was found to be able to regulate the DSB repair pathways in GV, GVBD, and MII oocytes. In the about 200 targets of CDK1 [49], in addition to RAD51 and RAD52 [7], DSB repair enzymes like MRE11 and CtIP are also regulated by CDK1 [50, 51], indicating that CDK1 plays essential roles in DSB repair and may affect chromosome stability through impairing DSB repair. In addition, the classic function of CDK1 is to control the cell cycle and chromosome segregation, so chromosome number instability could also be directly caused by CDK1 deficiency [52, 53]. As features of oocyte are inherited by early embryos, it can be speculated that CDK1 may play a key role in the formation of early embryonic aneuploidy and should be monitored during gamete or embryo development.

Culture conditions in gametes and early embryos may not only affect the genome stability but also affect epigenome stability [54]. Pyruvate deprivation in culture medium would constrict nucleus localization of tricarboxylic acid cycle enzymes and alter histone modifications in early embryos [55]. Interfering of pyruvate metabolism during IVM would alter the histone acetylation level at H3K9 in bovine oocytes [56]. High concentration of glucose could affect the DNA methylation at *PEG3* gene in human IVM oocytes [57]. All these data above indicated that metabolic micro-environment changes could induce epigenetic changes in gametes and embryos and make them weaker in developmental ability or carry unhealthy factors. In this study, we linked metabolites in the culture medium to CDK1 protein level and DSB repair. In embryonic stem cells, epigenetic regulators are phosphorylation targets of CDK1, and alteration of CDK1 activity would affect the global epigenetic landscape [58]. And the DSB repair choices are affected by the pre-existing histone modifications, such as H4K16ac, as well as DSB induced modifications [59, 60]. Whether the epigenetic changes caused by metabolites is mediated by CDK1 and whether CDK1 also takes effects on DSB repair through histone modification are also worth our concern.

During human reproduction, complex genome rearrangement in gametes or embryos might cause rare diseases in human [61–63]. The complex genome rearrangements are very common in cancer cells [64] and can

be promoted by the template switching and BIR repair of DSBs [65–67]. In oocytes, we found BIR could be induced by DSBs in SN, GVBD, and MII stage oocytes but not in the NSN oocytes whose chromatin are less condensed [27]. As the high pathogenicity of complex genome rearrangement, the DSBs as well as BIR pathway should be avoided during IVM, and regulating BIR from the perspective of metabolites may be a potential approach.

Conclusions

This work reveals that the DSB repair in MII oocytes is regulated by the CDK1 activity and oocyte metabolic micro-environment. CDK1 promotes BIR and RAD51-mediated HDR but suppress the TMEJ, whereas high energic media promote TMEJ but suppress BIR and RAD51-mediated HDR. Oocyte in vitro maturation media have no obvious effect on 53BP1-mediated NHEJ.

Methods

Oocyte collection and in vitro maturation

All animal manipulations in this study were approved by the Ethics Committee of Guangdong Second Provincial General Hospital. The oocytes used in this study were isolated from 8- to 12-week-old female ICR strain mice. To isolate GV oocytes, mouse ovaries were chopped and dispersed in M2 medium (Sigma, M7167). To isolate CEOs, 10 IU of PMSG was injected into mice, and the CEOs were isolated from mouse ovaries 48 h after PMSG injection. The denuded oocytes were squeezed from surrounding cumulus cells by a mouth pipette. To block GV-stage oocytes from GVBD, 2.5 μM milrinone (MCE, HY-14252) was added to M2 medium for oocyte manipulation. To isolate in vivo oocytes at different maturation stages, mice were injected with 10 IU of hCG 48 h after PMSG injection. In vivo GVBD oocytes were isolated from ovaries at 2 h after hCG injection. Cumulus-oocyte complexes were collected from oviducts 14 h after hCG injection, and in vivo generated MII oocytes were isolated from cumulus-oocyte complexes via hyaluronidase (Sangon, A600503) treatment.

For in vitro maturation of GV oocytes, the oocytes were washed with M2 medium 3 times to remove Milrinone and then cultured in different media covered with mineral oil (Sigma, M8410) until the end of the experiment. In this study, the media used for IVM were M2, DMEM (Sangon, E600003; with 10% FBS, Tocyto, UT81304), M2 + Gl (M2 + 1% (v/v) of 0.3 g/ml glucose), M2 + Py (M2 + 1% (v/v) of 0.0144 g/ml sodium pyruvate), M2 + FBS (M2 + 10% FBS), M2 + G.P. (M2 + glucose + pyruvate), M2 + G.P.F. (M2 + glucose + pyruvate + 10% FBS), and M2plus (M2 + glucose + pyruvate + pyruvate + 10% FBS + 1 × essential amino acid (Procell, PB180425) + 1 × nonessential amino acid (Procell, PB180424)).

Chemical agent treatments of oocytes

In this study, DSBs in oocytes were induced by a 1-h treatment with 10 μM Bleomycin (Selleck, S1214). To suppress the activity of CDK1 in oocytes at the GV stage, 10 μM RO-3306 (MCE, HY-12529) was used to treat the oocytes throughout the course of the experiment. To suppress CDK1 in IVM 2 h, IVM 12 h, or IVM 14 h oocytes, the oocytes were first cultured for 2 h or 14 h and then treated with 10 μM RO-3306 for the following experiments. To block the activity of BRCA1, 100 μM Bractoppin (MCE, HY-126020) was used to treat oocytes. To block DNA polymerases, Aphidicolin (Glpbio, GC10867) was used to treat the oocytes throughout the course of the experiment. In these chemical agent treatment experiments, DMSO (MCE, HY-Y0320) was used as the control agent.

Immunofluorescence labeling

For immunofluorescence labeling, the oocytes were fixed with 4% paraformaldehyde and permeabilized with 0.3% Triton X-100 for 15 and 20 min at room temperature (RT). To denature oocyte proteins such as POLQ and RAD51, the oocytes were treated with Quick Antigen Retrieval Solution for Frozen Sections (Beyotime, P0090) for 30 min at RT. Then, the oocytes were blocked in PBST (0.1% Tween-20 in PBS) supplemented with 1% bovine serum albumin (Sangon, A600332) for 30 min at RT and incubated with primary antibody (1:100–1:200 dilution in blocking buffer) overnight at 4 °C. After 5 washes with PBST, the oocytes were incubated in PBST with secondary antibody for 3 h at RT. Then, the oocytes were washed with PBST 5 times and mounted with Antifade Mounting Medium supplemented with DAPI (Beyotime, P0131). An Andor Dragonfly Confocal Microscope System was used for oocyte immunofluorescence image capture. All image data were analyzed using the Image J software [68]. The primary antibodies used in this study were anti-γH2AX (Bioworlde, BS4760), anti-tubulin (Tubulin-Tracker Red, Beyotime, C1050), anti-GFP (Abbkine, ABT2020), anti-RAD51 (Zen-bio, 200,514), and anti-POLQ (Sangon, D263727).

EdU click reaction

To label the newly synthesized DNA in the oocytes, 10 μM EdU (Beyotime, ST067) was added to the culture medium during the experiments. The EdU click reaction was performed according to the instructions of the EdU Cell Proliferation Kit with Alexa Fluor 488 (Beyotime, C0071S). In brief, the oocytes were first fixed in PBS supplemented with 4% paraformaldehyde for 15 min and then permeabilized in PBS supplemented with 0.3% Triton X-100 for 20 min at RT. After immunofluorescence labeling, if needed, the oocytes were treated with click reaction buffer at RT for 1 h and then washed with PBST

5 times. Then, the oocytes were mounted with Antifade Mounting Medium supplemented with DAPI.

Western blot

To compare the protein levels in different groups of oocytes, 50 oocytes in 10 μL of M2 medium from each group were added to 2 μL of 5 × SDS–PAGE sample loading buffer and boiled for 5 min. Then, the samples were centrifuged and used for Western blotting. The proteins were transferred onto 0.2 μm PVDF membranes (Beyotime, FFP24) and labeled with primary and secondary antibodies. The primary antibodies used in this study were anti-CDK1 (Proteintech, 67,575–1-Ig), anti-CCNB1 (Abcam, Ab181593), and anti-Cofilin (Abcam, 66,057–1-Ig) as internal reference proteins. After antibody incubation and washing, the protein bands were detected using an enhanced chemiluminescence reagent kit (Vazyme, E412) with a Bio-Rad ChemiDoc system. All western blot results were repeated for three times.

cRNA preparation and oocyte microinjection

The CDS regions of mouse *CDK1*, *RAD51* and *53BP1* were amplified from mouse ovarian cDNAs. Then, the CDSs were recombined into the multiple cloning sites of the pmCherry-N1 or pEGFP-C1 vector with a Seamless Cloning Kit (Beyotime, D7010). The recombinant *CDK1-mCherry*, *GFP-RAD51*, and *GFP-53BP1* plasmids were transformed into *E. coli*, and the sequences were identified by bacterial plasmid sequencing. Then, the sequences expressing recombinant proteins and the *EGFP* gene in pEGFP-C1 were amplified using the following primer pairs: forward primer, GTGAATTGTA ATACGACTCA CTATAGGGCA GGT CTATATA AGCAGAGCT, which contains a T7 promoter, and reverse primer, AATATTAACG CTTACAATTT. The mouse *CCNB1* CDS linked with *mVenus* coding sequence was insert into the pcDNA3.1 vector, and the *CCNB1-mVenus* gene was amplified by primers: forward primer, CTCTCTGGCT AACTAGAGAA CC, and reverse primer, GGGGATACCC CCTAGAGC. The amplified PCR products were purified using a QIAquick PCR Purification Kit (Qiagen, 28,104) and transcribed in vitro into cRNAs with a HiScribe T7 ARCA mRNA Kit (NEB, E2060).

The cRNAs were injected into oocytes using the Eppendorf PiezoXpert system. For the *GFP-RAD51* or *GFP-53BP1* cRNAs, GV-stage oocytes blocked in medium supplemented with Milrinone were treated with bleomycin 3 h after cRNA injection. For the IVM 2 h oocytes, cRNAs were injected into the Milrinone-blocked GV stage oocytes, and then these oocytes were released from Milrinone and cultured in vitro for 2 h and treated with Bleomycin for 1 h. For the IVM 14 h oocytes, the oocytes that had extruded PB1 were injected with cRNAs, maintained in medium for 1 h, and then treated with Bleomycin. As the GFP structures could be destroyed by the click reaction, when both the EdU and GFP-RAD51 needed to be detected, the GFP-RAD51 signals were further detected using GFP antibodies.

For the *EGFP*, *CCNB1-mVenus*, and *CDK1-mCherry* cRNAs, they were injected into Milrinone blocked GV-stage oocytes for 8 h to observe the GVBD of oocytes. The expression of fluorescent proteins was detected by couple-charged device camera 3 h after micro-injection. These cRNAs were also injected into the M2 + G.P.F. medium matured MII oocytes. After injection for 3 h, these oocytes were treated with Bleomycin for 1 h and released from Bleomycin for 6 h to analyze the effects of exogenous proteins on oocyte DSB repair.

Statistics

In this study, the significance of the differences in proportions between different groups was analyzed using Fisher's exact test. The mean values were firstly analyzed by Shapiro–Wilk normality test and Levene's test. Then, ANOVA combined with Tukey HSD test or Tukey–Kramer-Nemenyi test was used to analyze the significance of differences in means between different groups. All statistical analysis were performed using the R software (https://www.r-project.org/). p values < 0.01 indicated very significant differences (**), p values < 0.05 and > 0.01 indicated significant differences (*), and p values > 0.05 indicated nonsignificant differences. To count the protein focus numbers or volumes in the oocytes, the oocyte immunofluorescence labeling images were scanned using the Z-scan method in the Andor Dragonfly confocal system, and the number and volume of foci were analyzed using the Image J software.

Abbreviations

IVM	In vitro maturation
GV	Germinal vesicle
GVBD	Germinal vesicle breakdown
MI	Metaphase of the first meiosis
MII	Metaphase of the second meiosis
CEO	Cumulus cells enclosed oocyte
DO	Denuded oocyte
DSB	Double-strand break
HDR	Homology-directed repair
NHEJ	Nonhomologous end joining
BIR	Break-induced replication
TMEJ	Polymerase theta-mediated end joining

Acknowledgements

We thank all the members at the Clinical Lab and Fertility Preservation Lab of the Reproductive Medicine Center at Guangdong Second Provincial General Hospital for their support of this study.

Authors' contributions

Conceptualization: JYM, XHO, QYS and SY; formal analysis: TJX and JYM; funding acquisition: JYM and SY; investigation: TX, XGZ, JC, SL and FYX; methodology: JYM and QZ; project administration: JYM; visualization: JYM and TJX; writing: JYM and TJX. All authors read and approved the final manuscript.

Funding
This work is supported by the National Key R&D Program of China (2022YFC2703200), the National Natural Science Foundation of China (82271683), the Guangzhou Basic Research Program project (2023A03J0255), and the Shandong Provincial Natural Science Foundation (ZR2022MC080).

Data availability
All data generated or analyzed during this study are included in this published article.

Declarations

Ethics approval and consent to participate
All animal manipulations were approved by the Ethics Committee of Guangdong Second Provincial General Hospital (Approval No. 2023-DW-KZ-050–02).

Content for publication
Not applicable.

Competing interests
The authors declare that they have no competing interests.

Received: 7 April 2024 Accepted: 23 January 2025
Published online: 06 February 2025

References

1. Scully R, Panday A, Elango R, Willis NA. DNA double-strand break repair-pathway choice in somatic mammalian cells. Nat Rev Mol Cell Biol. 2019;20(11):698–714.
2. Takata M, Sasaki MS, Sonoda E, Morrison C, Hashimoto M, Utsumi H, Yamaguchi-Iwai Y, Shinohara A, Takeda S. Homologous recombination and non-homologous end-joining pathways of DNA double-strand break repair have overlapping roles in the maintenance of chromosomal integrity in vertebrate cells. EMBO J. 1998;17(18):5497–508.
3. Daley JM, Sung P. 53BP1, BRCA1, and the choice between recombination and end joining at DNA double-strand breaks. Mol Cell Biol. 2014;34(8):1380–8.
4. Escribano-Diaz C, Orthwein A, Fradet-Turcotte A, Xing M, Young JT, Tkac J, Cook MA, Rosebrock AP, Munro M, Canny MD, et al. A cell cycle-dependent regulatory circuit composed of 53BP1-RIF1 and BRCA1-CtIP controls DNA repair pathway choice. Mol Cell. 2013;49(5):872–83.
5. Johnson N, Cai D, Kennedy RD, Pathania S, Arora M, Li YC, D'Andrea AD, Parvin JD, Shapiro GI. Cdk1 participates in BRCA1-dependent S phase checkpoint control in response to DNA damage. Mol Cell. 2009;35(3):327–39.
6. Martinez-Alonso D, Malumbres M. Mammalian cell cycle cyclins. Semin Cell Dev Biol. 2020;107:28–35.
7. Lim G, Chang Y, Huh WK. Phosphoregulation of Rad51/Rad52 by CDK1 functions as a molecular switch for cell cycle-specific activation of homologous recombination. Sci Adv. 2020;6(6):eaay2669.
8. Ramsden DA, Carvajal-Garcia J, Gupta GP. Mechanism, cellular functions and cancer roles of polymerase-theta-mediated DNA end joining. Nat Rev Mol Cell Biol. 2022;23(2):125–40.
9. Kramara J, Osia B, Malkova A. Break-induced replication: the where, the why, and the how. Trends Genet. 2018;34(7):518–31.
10. Bakr A, Kocher S, Volquardsen J, Reimer R, Borgmann K, Dikomey E, Rothkamm K, Mansour WY. Functional crosstalk between DNA damage response proteins 53BP1 and BRCA1 regulates double strand break repair choice. Radiother Oncol. 2016;119(2):276–81.
11. Milholland B, Dong X, Zhang L, Hao X, Suh Y, Vijg J. Differences between germline and somatic mutation rates in humans and mice. Nat Commun. 2017;8:15183.
12. Shukla V, Hoffding MK, Hoffmann ER. Genome diversity and instability in human germ cells and preimplantation embryos. Semin Cell Dev Biol. 2021;113:132–47.
13. Ma JY, Xia TJ, Li S, Yin S, Luo SM, Li G. Germline cell de novo mutations and potential effects of inflammation on germline cell genome stability. Semin Cell Dev Biol. 2024;154(Pt C):316–27.
14. Ma JY, Feng X, Tian XY, Chen LN, Fan XY, Guo L, Li S, Yin S, Luo SM, Ou XH. The repair of endo/exogenous DNA double-strand breaks and its effects on meiotic chromosome segregation in oocytes. Hum Mol Genet. 2019;28(20):3422–30.
15. Yang Q, Xi Q, Wang M, Liu J, Li Z, Hu J, Jin L, Zhu L. Rapamycin improves the developmental competence of human oocytes by alleviating DNA damage during IVM. Hum Reprod Open. 2022;2022(4):hoac050.
16. Chian RC, Uzelac PS, Nargund G. In vitro maturation of human immature oocytes for fertility preservation. Fertil Steril. 2013;99(5):1173–81.
17. Chian RC, Li JH, Lim JH, Yoshida H. IVM of human immature oocytes for infertility treatment and fertility preservation. Reprod Med Biol. 2023;22(1):e12524.
18. Li XM, Yu C, Wang ZW, Zhang YL, Liu XM, Zhou D, Sun QY, Fan HY. DNA topoisomerase II is dispensable for oocyte meiotic resumption but is essential for meiotic chromosome condensation and separation in mice. Biol Reprod. 2013;89(5):118.
19. He DJ, Wang L, Zhang ZB, Guo K, Li JZ, He XC, Cui QH, Zheng P. Maternal gene Ooep may participate in homologous recombination-mediated DNA double-strand break repair in mouse oocytes. Zool Res. 2018;39(6):387–95.
20. Marangos P, Carroll J. Oocytes progress beyond prophase in the presence of DNA damage. Curr Biol. 2012;22(11):989–94.
21. Lee C, Leem J, Oh JS. Selective utilization of non-homologous end-joining and homologous recombination for DNA repair during meiotic maturation in mouse oocytes. Cell Prolif. 2023;56(4):e13384.
22. Leem J, Kim JS, Oh JS. Oocytes can repair DNA damage during meiosis via a microtubule-dependent recruitment of CIP2A-MDC1-TOPBP1 complex from spindle pole to chromosomes. Nucleic Acids Res. 2023;51(10):4899–913.
23. Li J, Qian WP, Sun QY. Cyclins regulating oocyte meiotic cell cycle progressiondagger. Biol Reprod. 2019;101(5):878–81.
24. Levasseur MD, Thomas C, Davies OR, Higgins JMG, Madgwick S. Aneuploidy in oocytes is prevented by sustained CDK1 activity through degron masking in cyclin B1. Dev Cell. 2019;48(5):672-684 e675.
25. Jacobs K, Zambelli F, Mertzanidou A, Smolders I, Geens M, Nguyen HT, Barbe L, Sermon K, Spits C. Higher-density culture in human embryonic stem cells results in DNA damage and genome instability. Stem Cell Reports. 2016;6(3):330–41.
26. Prakash Bangalore M, Adhikarla S, Mukherjee O, Panicker MM. Genotoxic effects of culture media on human pluripotent stem cells. Sci Rep. 2017;7:42222.
27. Ma JY, Feng X, Xie FY, Li S, Chen LN, Luo SM, Yin S, Ou XH. Double-strand breaks induce short-scale DNA replication and damage amplification in the fully grown mouse oocytes. Genetics. 2021;218(2):iyab054.
28. Sutton-McDowall ML, Gilchrist RB, Thompson JG. The pivotal role of glucose metabolism in determining oocyte developmental competence. Reproduction. 2010;139(4):685–95.
29. Sun MH, Zheng J, Xie FY, Shen W, Yin S, Ma JY. Cumulus cells block oocyte meiotic resumption via gap junctions in cumulus oocyte complexes subjected to DNA double-strand breaks. PLoS ONE. 2015;10(11):e0143223.
30. Shindo M, Miyado K, Kang W, Fukami M, Miyado M. Efficient superovulation and egg collection from mice. Bio Protoc. 2022;12(11):e4439.
31. Wassing IE, Graham E, Saayman X, Rampazzo L, Ralf C, Bassett A, Esashi F. The RAD51 recombinase protects mitotic chromatin in human cells. Nat Commun. 2021;12(1):5380.
32. Vassilev LT, Tovar C, Chen S, Knezevic D, Zhao X, Sun H, Heimbrook DC, Chen L. Selective small-molecule inhibitor reveals critical mitotic functions of human CDK1. Proc Natl Acad Sci U S A. 2006;103(28):10660–5.
33. Adhikari D, Diril MK, Busayavalasa K, Risal S, Nakagawa S, Lindkvist R, Shen Y, Coppola V, Tessarollo L, Kudo NR, et al. Mastl is required for timely activation of APC/C in meiosis I and Cdk1 reactivation in meiosis II. J Cell Biol. 2014;206(7):843–53.
34. Gelot C, Kovacs MT, Miron S, Mylne E, Haan A, Boeffard-Dosierre L, Ghouil R, Popova T, Dingli F, Loew D, et al. Poltheta is phosphorylated by PLK1 to repair double-strand breaks in mitosis. Nature. 2023;621(7978):415–22.
35. Orthwein A, Fradet-Turcotte A, Noordermeer SM, Canny MD, Brun CM, Strecker J, Escribano-Diaz C, Durocher D. Mitosis inhibits DNA double-strand break repair to guard against telomere fusions. Science. 2014;344(6180):189–93.

36. Nothias JY, Majumder S, Kaneko KJ, DePamphilis ML. Regulation of gene expression at the beginning of mammalian development. J Biol Chem. 1995;270(38):22077–80.
37. Knoblochova L, Duricek T, Vaskovicova M, Zorzompokou C, Rayova D, Ferencova I, Baran V, Schultz RM, Hoffmann ER, Drutovic D. CHK1-CDC25A-CDK1 regulate cell cycle progression and protect genome integrity in early mouse embryos. EMBO Rep. 2023;24(10):e56530.
38. Simon L, Murphy K, Shamsi MB, Liu L, Emery B, Aston KI, Hotaling J, Carrell DT. Paternal influence of sperm DNA integrity on early embryonic development. Hum Reprod. 2014;29(11):2402–12.
39. Kort DH, Chia G, Treff NR, Tanaka AJ, Xing T, Vensand LB, Micucci S, Prosser R, Lobo RA, Sauer MV, et al. Human embryos commonly form abnormal nuclei during development: a mechanism of DNA damage, embryonic aneuploidy, and developmental arrest. Hum Reprod. 2016;31(2):312–23.
40. Bohrer RC, Coutinho AR, Duggavathi R, Bordignon V. The incidence of DNA double-strand breaks is higher in late-cleaving and less developmentally competent porcine embryos. Biol Reprod. 2015;93(3):59.
41. Han L, Ren C, Li L, Li X, Ge J, Wang H, Miao YL, Guo X, Moley KH, Shu W, et al. Embryonic defects induced by maternal obesity in mice derive from Stella insufficiency in oocytes. Nat Genet. 2018;50(3):432–42.
42. Luna M, Copperman AB, Duke M, Ezcurra D, Sandler B, Barritt J. Human blastocyst morphological quality is significantly improved in embryos classified as fast on day 3 (>or=10 cells), bringing into question current embryological dogma. Fertil Steril. 2008;89(2):358–63.
43. Lundin K, Bergh C, Hardarson T. Early embryo cleavage is a strong indicator of embryo quality in human IVF. Hum Reprod. 2001;16(12):2652–7.
44. Lee YSL, Gardner DK. Early cleaving embryos result in blastocysts with increased aspartate and glucose consumption, which exhibit different metabolic gene expression that persists in placental and fetal tissues. J Assist Reprod Genet. 2021;38(12):3099–111.
45. Palmerola KL, Amrane S, De Los Angeles A, Xu S, Wang N, de Pinho J, Zuccaro MV, Taglialatela A, Massey DJ, Turocy J, et al. Replication stress impairs chromosome segregation and preimplantation development in human embryos. Cell. 2022;185(16):2988–3007.
46. Zhai F, Kong S, Song S, Guo Q, Ding L, Zhang J, Wang N, Kuo Y, Guan S, Yuan P, et al. Human embryos harbor complex mosaicism with broad presence of aneuploid cells during early development. Cell Discov. 2024;10(1):98.
47. Wang Y, Wang Z, Wu X, Ling X, Zhang J, Liu M. Clinical outcomes of subtypes of mosaic single aneuploid embryos after preimplantation genetic testing for aneuploidy. J Assist Reprod Genet. 2023;40(3):639–52.
48. Waldvogel SM, Posey JE, Goodell MA. Human embryonic genetic mosaicism and its effects on development and disease. Nat Rev Genet. 2024;25(10):698–714.
49. Ubersax JA, Woodbury EL, Quang PN, Paraz M, Blethrow JD, Shah K, Shokat KM, Morgan DO. Targets of the cyclin-dependent kinase Cdk1. Nature. 2003;425(6960):859–64.
50. Simoneau A, Robellet X, Ladouceur AM, D'Amours D. Cdk1-dependent regulation of the Mre11 complex couples DNA repair pathways to cell cycle progression. Cell Cycle. 2014;13(7):1078–90.
51. Peterson SE, Li Y, Chait BT, Gottesman ME, Baer R, Gautier J. Cdk1 uncouples CtIP-dependent resection and Rad51 filament formation during M-phase double-strand break repair. J Cell Biol. 2011;194(5):705–20.
52. Valles SY, Bural S, Godek KM, Compton DA. Cyclin A/Cdk1 promotes chromosome alignment and timely mitotic progression. Mol Biol Cell. 2024;35(11):ar141.
53. Li J, Ouyang YC, Zhang CH, Qian WP, Sun QY. The cyclin B2/CDK1 complex inhibits separase activity in mouse oocyte meiosis I. Development. 2019;146(23):dev182519.
54. Calle A, Fernandez-Gonzalez R, Ramos-Ibeas P, Laguna-Barraza R, Perez-Cerezales S, Bermejo-Alvarez P, Ramirez MA, Gutierrez-Adan A. Long-term and transgenerational effects of in vitro culture on mouse embryos. Theriogenology. 2012;77(4):785–93.
55. Nagaraj R, Sharpley MS, Chi F, Braas D, Zhou Y, Kim R, Clark AT, Banerjee U. Nuclear localization of mitochondrial TCA cycle enzymes as a critical step in mammalian zygotic genome activation. Cell. 2017;168(1–2):210-223 e211.
56. da AlcantaraSilva JV. Ispada J, Nociti RP, da Fonseca Junior AM, de Lima CB, Dos Santos EC, Chiaratti MR, Milazzotto MP: The central role of pyruvate metabolism on the epigenetic maturation and transcriptional profile of bovine oocytes. Reproduction. 2024;167(4):e230181.
57. Wang Q, Tang SB, Song XB, Deng TF, Zhang TT, Yin S, Luo SM, Shen W, Zhang CL, Ge ZJ. High-glucose concentrations change DNA methylation levels in human IVM oocytes. Hum Reprod. 2018;33(3):474–81.
58. Michowski W, Chick JM, Chu C, Kolodziejczyk A, Wang Y, Suski JM, Abraham B, Anders L, Day D, Dunkl LM, et al. Cdk1 controls global epigenetic landscape in embryonic stem cells. Mol Cell. 2020;78(3):459-476 e413.
59. Vergara X, Manjon AG, de Haas M, Morris B, Schep R, Leemans C, Friskes A, Beijersbergen RL, Sanders MA, Medema RH, et al. Widespread chromatin context-dependencies of DNA double-strand break repair proteins. Nat Commun. 2024;15(1):5334.
60. Horikoshi N, Sharma D, Leonard F, Pandita RK, Charaka VK, Hambarde S, Horikoshi NT, Gaur Khaitan P, Chakraborty S, Cote J, et al. Pre-existing H4K16ac levels in euchromatin drive DNA repair by homologous recombination in S-phase. Commun Biol. 2019;2:253.
61. Bertelsen B, Nazaryan-Petersen L, Sun W, Mehrjouy MM, Xie G, Chen W, Hjermind LE, Taschner PE, Tumer Z. A germline chromothripsis event stably segregating in 11 individuals through three generations. Genet Med. 2016;18(5):494–500.
62. Trpchevska N, Dimova I, Arabadji T, Milachich T, Angelova S, Dimitrova M, Hristova-Savova M, Andreeva P, Timeva T, Shterev A. A family study of complex chromosome rearrangement involving chromosomes 1, 8, and 11 and its reproductive consequences. J Assist Reprod Genet. 2017;34(5):659–69.
63. Schuy J, Grochowski CM, Carvalho CMB, Lindstrand A. Complex genomic rearrangements: an underestimated cause of rare diseases. Trends Genet. 2022;38(11):1134–46.
64. Li Y, Roberts ND, Wala JA, Shapira O, Schumacher SE, Kumar K, Khurana E, Waszak S, Korbel JO, Haber JE, et al. Patterns of somatic structural variation in human cancer genomes. Nature. 2020;578(7793):112–21.
65. Sakofsky CJ, Ayyar S, Deem AK, Chung WH, Ira G, Malkova A. Translesion polymerases drive microhomology-mediated break-induced replication leading to complex chromosomal rearrangements. Mol Cell. 2015;60(6):860–72.
66. Costantino L, Sotiriou SK, Rantala JK, Magin S, Mladenov E, Helleday T, Haber JE, Iliakis G, Kallioniemi OP, Halazonetis TD. Break-induced replication repair of damaged forks induces genomic duplications in human cells. Science. 2014;343(6166):88–91.
67. Piazza A, Wright WD, Heyer WD. Multi-invasions are recombination byproducts that induce chromosomal rearrangements. Cell. 2017;170(4):760-773 e715.
68. Schindelin J, Arganda-Carreras I, Frise E, Kaynig V, Longair M, Pietzsch T, Preibisch S, Rueden C, Saalfeld S, Schmid B, et al. Fiji: an open-source platform for biological-image analysis. Nat Methods. 2012;9(7):676–82.

Publisher's Note